Composites Science and Technology 152 (2017) 101–110

Contents lists available at ScienceDirect

Composites Science and Technology

journal homepage: http://www.elsevier.com/locate/compscitech

High performance quasi-isotropic thin-ply carbon/glass hybrid composites with pseudo-ductile behaviour in all fibre orientations

Mohamad Fotouhi [a, b, *], Meisam Jalalvand [c, b], Michael R. Wisnom [b]

[a] Department of Design and Mathematics, University of the West of England, Bristol BS16 1QY, UK
[b] Bristol Composites Institute (ACCIS), University of Bristol, Bristol BS8 1TR, UK
[c] Department of Mechanical and Aerospace Engineering, The University of Strathclyde, 75 Montrose Street, Glasgow G1 1XJ, UK

ARTICLE INFO

Article history:
Received 26 May 2017
Received in revised form
19 August 2017
Accepted 21 August 2017
Available online 24 August 2017

Keywords:
Carbon fibres
Glass fibres
Thin-ply
Hybrid composites
Delamination
Fragmentation

ABSTRACT

This study exploits the potential of thin-ply carbon/glass hybrid laminates to generate high performance Quasi-Isotropic (QI) composite plates that show pseudo-ductility in all fibre orientations under tensile loading, overcoming the inherent brittleness of conventional composites. Two types of QI lay-ups with 45° and 60° intervals, i.e. [45/90/-45/0] and [60/-60/0], were used to fabricate novel architectures of a QI T300-carbon laminate sandwiched between the two halves of a QI S-glass laminate. The fabricated plates were then loaded in all their fibre orientations. The laminates were designed by choosing an appropriate ratio of the carbon thickness to the laminate thickness using a robust analytical damage mode map. The experimental results verified the analytical predictions and showed a desirable pseudo-ductile failure in all the fibre orientations. Microscope images taken through the laminates thickness showed fragmentations (fibre fractures in the carbon layer) appearing only in the 0° carbon plies. A hybrid effect was observed, with an increase in strain and stress to failure of the carbon fibres, which was found to be dependent on the stiffness of the plies separating the 0° carbon plies and the plies adjacent to the 0° carbon plies. Altering the stacking sequence changes the stiffness of the separator and adjacent plies, therefore, leads to changes in the pseudo-ductile characteristics such as the initiation and final failure strains.

1. Introduction

Polymer-matrix composites use has been continuously increased in engineering applications due to their superior mechanical properties. However, polymer composites show sudden brittle failure, with linear elastic response and little warning before failure. This drawback leads to large values of safety factors in their design.

Hybridisation of different types of fibres is one of the methods that can introduce gradual failure in composite materials [1–13]. Possible failure modes in a three-layer Uni-Directional (UD) hybrid laminate made from High Strain Material (HSM) and Low Strain Material (LSM) are illustrated schematically in Fig. 1. Two types of catastrophic failure modes occur in conventional hybrid composites; a) a single crack through the whole thickness of the laminate due to a high ratio of LSM to HSM thickness (improperly sized hybrid laminate), which results in a linear stress-strain curve (Fig. 1a, and b) a single fracture in the LSM instantaneously followed by unstable delamination, which appears on the stress–-strain graphs as a significant load drop (Fig. 1b). This is a typical failure mode in conventional standard ply thickness hybrid laminates. Fig. 1c shows a desired gradual failure where delamination is suppressed and multiple LSM fractures are obtained followed by stable localised pull-out. This desired pseudo-ductile behaviour is achievable by selecting appropriate material properties, appropriate values of relative thickness (i.e. proportion of the LSM to HSM) and absolute thickness of the LSM. Thin carbon plies have superior mechanical properties and lower energy release rates, delaying the propagation of intra- and interlaminar cracks [14–16]. Recently, thin-ply UD and QI hybrids with different types of low strain and high strain fibres were introduced that generated the desired nonlinear stress–strain response and pseudo-ductility that avoids the catastrophic failure in laminated composites [17–19].

Fig. 2 shows four main features of a pseudo-ductile laminate with a thin layer of low strain fibre plies; (i) Pseudo-yield strain

* Corresponding author. Department of Design and Mathematics, University of the West of England, Bristol BS16 1QY, UK.
E-mail address: m.fotouhi@bristol.ac.uk (M. Fotouhi).

https://doi.org/10.1016/j.compscitech.2017.08.024

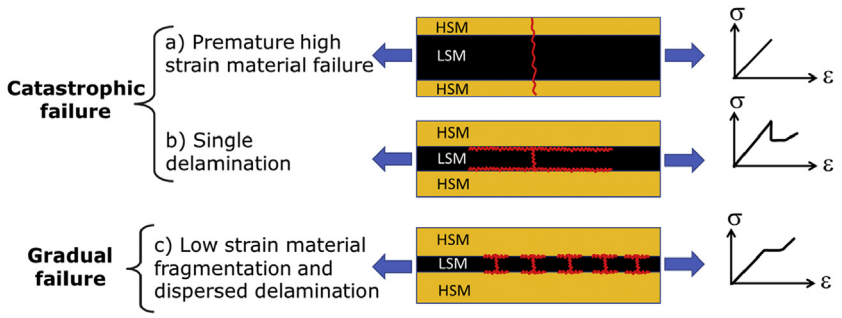

Fig. 1. Possible failure modes in a three layer UD hybrid made from HSM and LSM (red lines show fracture) (a) single crack through the whole specimen, (b) single crack in the LSM followed by instantaneous delamination, and (c) multiple fracture and localised stable pull-out of the LSM. (For interpretation of the references to colour in this figure legend, the reader is referred to the web version of this article.)

(ε_{py}), (ii) final failure strain (ε_f), (iii) Pseudo-ductile strain (ε_{pd}) and (iv) Hybrid effect. ε_{py} and σ_{py} are the strain and stress levels at which the tensile response deviates from the initial linear elastic behaviour, respectively. ε_f and σ_f are the final failure strain and stress values at which the HSM cannot carry any more load, respectively. It usually corresponds with fibre failure in the high strain material. Pseudo-ductile strain is the enhancement in strain achieved as a result of gradual failure and is calculated as the difference between the final failure strain, and the elastic strain based on the initial modulus at the final failure stress.

Hybrid effects were reported by different researchers [9–11], where they observed higher strain to failure of carbon in their UD glass/carbon hybrids than that of all carbon specimens. Swolfs et al. [20] reviewed the basic mechanisms causing the hybrid effect, with the most significant considered to be thermal residual stresses, altered failure development due to statistical effects on formation of clusters of fibre breaks and dynamic stress concentrations. Wisnom et al. [21] used glass/carbon hybrid composites, rather than all carbon composites, to measure the strain to failure of the baseline carbon plies more accurately, to reduce the variability typically obtained using conventional unidirectional tests and avoid the high values for the hybrid effect values when using these tests as the baseline [9–11]. This method addressed the difficulty in measuring the strain to failure due to stress concentrations at the load introduction regions. They defined hybrid effect as the enhancement in strain and stress to failure of the low strain fibres in the thin-ply hybrid composite, compared to those obtained in hybrid specimens with thick carbon plies where it was found that there is no hybrid effect.

The performance of the pseudo-ductile QI layups is influenced not only by the UD laminates' design parameters, but also by the stacking sequence of the plies. Recently, two different stacking approaches were used to fabricate pseudo-ductile hybrids to make a QI hybrid laminate; (i) orientation-blocked method, where the hybrid laminates were fabricated from optimised UD hybrid sub-laminates [22] and (ii) orientation-dispersed method in which the hybrid laminates were made from different non-hybrid multi-directional sub-laminates [23]. A nonlinear stress–strain response was achieved in both cases, however, using the orientation-blocked concept, there were significant free-edge delaminations. The orientation-dispersed method is considerably better to decrease interlaminar stresses at the free-edges and to suppress free-edge delamination [23].

Previous studies indicated that the pseudo-ductility is achieved in the QI hybrids in one loading orientation when subjected to tension [22,23]. However, most composite structures are subjected to multiple loading orientations, therefore, the aim of this paper is to study the potential of thin-ply carbon/glass hybrid laminates and

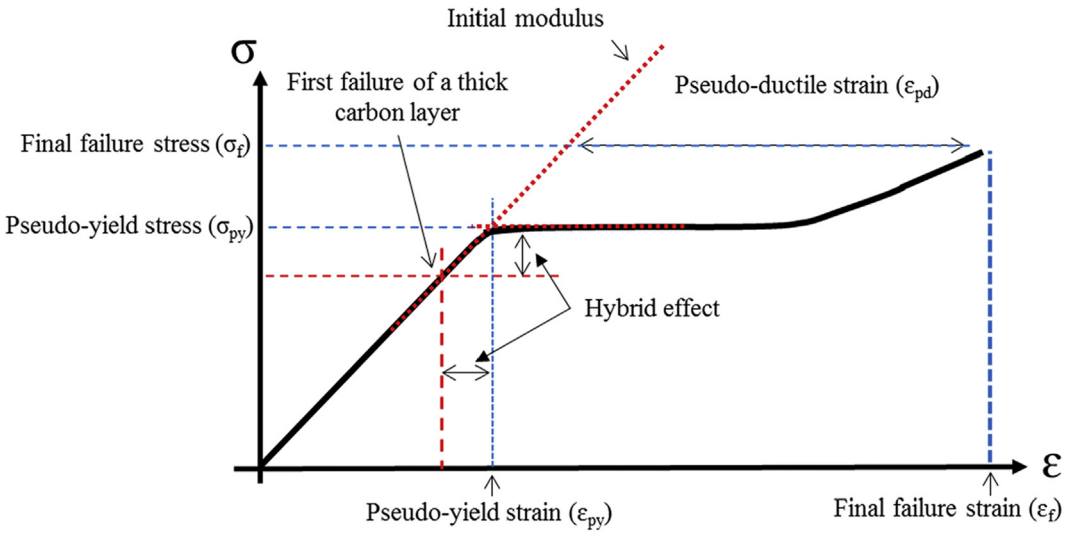

Fig. 2. Schematic of the stress–strain graph of a thin-ply hybrid with pseudo-ductility.

the orientation-dispersed method to generate high performance QI composite plates that show pseudo-ductility when loaded in all the fibres orientations under tension. Microscope images taken through the laminates thickness were used to detect fragmentation location and density in the investigated opaque pseudo-ductile laminates. The results show that the order of the plies and the distance between the 0° carbon and glass plies influenced the damage scenario, the free-edge delamination and the hybrid effect. Altering the stacking sequence influences the stiffness of the inner plies separating the 0° carbon plies and the plies adjacent to the 0° carbon plies, which leads to changes in the pseudo-yield strain and final failure stress/strain. The study introduces for the first time hybrids that fail in a gradual manner when loaded in different directions-avoiding catastrophic failure and free-edge delamination.

2. Experimental procedures

2.1. Materials and specimen design

As listed in Table 1, the HSM is standard thickness UD S-glass/913 epoxy prepreg supplied by Hexcel and the LSM is thin carbon prepreg (SkyFlex USN020A) from SK Chemicals (South Korea) that has T300 carbon fibres made by Toray. Please note that these are different from the TR30 fibres in prepreg with the same manufacturer's designation tested previously [19]. The corresponding matrix was SK Chemical's type K 50 epoxy resin. The resin systems in the hybrid laminates were 120 °C curing epoxies, which were found to be compatible.

Table 2 gives information about the hybrid specimen types and the sequences that they were laid up in two different configurations of QI lay-ups, i.e. ±45QI (45/90/-45/0) and ±60QI (60/-60/0). From Table 2 and as shown in Fig. 3, adding the specified angles to the orientation of each sub-laminate, in specimens of type 1 and type 5, produces the other ±60QI and ±45QI layups, when the 0 direction is defined as the loading direction. By changing the angles at which each of the two quasi-isotropic configurations was tested, the behaviour in all the fibre directions of both types of laminates can be studied.

The layups were chosen using appropriate values of relative thickness (i.e. proportion of the low strain fibre plies) and absolute thickness of the carbon fibre plies. Pseudo-ductile response is achieved by suppression of catastrophic delamination and appearance of damage modes of (i) fragmentation in the carbon plies and (ii) local delamination, before the final failure of the high strain glass plies. This has been done through using damage mode maps, similar to those for UD laminates [18]. These show how the damage depends on the relative and absolute thickness of the different materials. To do so, the multi-directional glass and carbon sub-laminates were assumed to be homogenised before crack development. Cracks are assumed to propagate through the thickness of the whole carbon epoxy laminate. The equivalent in-plane

Table 1
Characteristics of the prepregs and fibres applied.

Prepreg type	S-glass/epoxy [18]	USN020A (T300/epoxy) [17]
Fibre modulus E (GPa)	88	230[b]
Fibre failure strain (%)	5.5	1.5
Cured nominal thickness (mm)	0.155	0.029
Fibre mass per unit area (g/m^2)	190	21
Fibre volume fraction (%)	50.0	40.5
E1 (GPa)	45.7	101.7
E2 (GPa)	15.4[a]	6.0[c]
G12 (GPa)	4.34[a]	2.40[c]
V12	0.3[a]	0.3[c]
Equivalent in-plane stiffness for QI (GPa)	15.2	37.8

[a] Assumed to be equal to E-glass properties used in Ref. [24].
[b] This value is based on T300 Data Sheet [25].
[c] The transverse properties were assumed to be equal to the similar USN020A prepreg utilised in Ref. [26], as the data was not available.

Table 2
Layups of the investigated laminates, 0 plies highlighted in red.

Specimen type	Relative layup	Resulting layup
(1) = ±60QI/0°	(1)	$[60_{S\text{-}glass}/\text{-}60_{S\text{-}glass}/\underline{\boldsymbol{0}_{S\text{-}glass}}/\underline{\boldsymbol{0}_{C\text{-}T300}}/60_{C\text{-}T300}/\text{-}60_{C\text{-}T300}]_s$
(2) = ±60QI/+60°	(2) = (1) + 60°	$[\text{-}60_{S\text{-}glass}/\underline{\boldsymbol{0}_{S\text{-}glass}}/60_{S\text{-}glass}/60_{C\text{-}T300}/\text{-}60_{C\text{-}T300}/\underline{\boldsymbol{0}_{C\text{-}T300}}]_s$
(3) = ±60QI/-60°	(3) = (1) - 60°	$[\underline{\boldsymbol{0}_{S\text{-}glass}}/60_{S\text{-}glass}/\text{-}60_{S\text{-}glass}/\text{-}60_{C\text{-}T300}/\underline{\boldsymbol{0}_{C\text{-}T300}}/60_{C\text{-}T300}]_s$
(4) = ±45QI/0°	(4)	$[45_{S\text{-}glass}/90_{S\text{-}glass}/\text{-}45_{S\text{-}glass}/\underline{\boldsymbol{0}_{S\text{-}glass}}/\underline{\boldsymbol{0}_{C\text{-}T300}}/45_{C\text{-}T300}/90_{C\text{-}T300}/\text{-}45_{C\text{-}T300}]_s$
(5) = ±45QI/+45°	(5) = (4) + 45°	$[90_{S\text{-}glass}/\text{-}45_{S\text{-}glass}/\underline{\boldsymbol{0}_{S\text{-}glass}}/45_{S\text{-}glass}/45_{C\text{-}T300}/90_{C\text{-}T300}/\text{-}45_{C\text{-}T300}/\underline{\boldsymbol{0}_{C\text{-}T300}}]_s$
(6) = ±45QI/+90°	(6) = (4) + 90°	$[\text{-}45_{S\text{-}glass}/\underline{\boldsymbol{0}_{S\text{-}glass}}/45_{S\text{-}glass}/90_{S\text{-}glass}/90_{C\text{-}T300}/\text{-}45_{C\text{-}T300}/\underline{\boldsymbol{0}_{C\text{-}T300}}/45_{C\text{-}T300}]_s$
(7) = ±45 QI/-45°	(7) = (4) - 45°	$[\underline{\boldsymbol{0}_{S\text{-}glass}}/45_{S\text{-}glass}/90_{S\text{-}glass}/\text{-}45_{S\text{-}glass}/\text{-}45_{C\text{-}T300}/\underline{\boldsymbol{0}_{C\text{-}T300}}/45_{C\text{-}T300}/90_{C\text{-}T300}]_s$

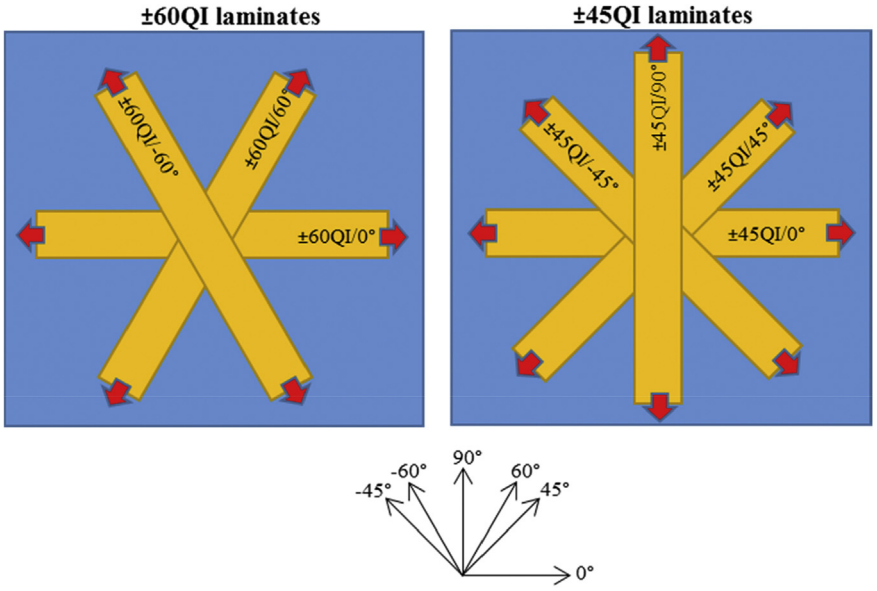

Fig. 3. Schematic of the investigated laminates in a QI composite plate, the red arrows showing the loading directions. (For interpretation of the references to colour in this figure legend, the reader is referred to the web version of this article.)

moduli of both glass and carbon QI laminates, calculated using Classical Laminate Theory, are given in Table 1. The failure strain of the homogenised materials is assumed to be equal to the fibre failure strain of the 0° layers. This is an acceptable assumption as the stiffness reduction in the deterioration process of the homogenised QI laminate is mainly due to 0° carbon layer fragmentation and the final failure of the QI glass is because of 0° layer glass failure. Although this assumption may not be completely accurate one due to hybrid effects, it is a reasonable basis to design the configurations. Most of the strength and stiffness of each layer is coming from the 0° layers and fragmentation/failure of this layer means a big drop in the stiffness of the remaining parts or failure of the whole laminate. Interfacial fracture toughness between the glass and carbon layers, G_{IIc}, was assumed to be 1 N/mm [18]. The damage mode map with calculated boundaries between the different regions is illustrated in Fig. 4, for the investigated ±60QI and ±45QI specimens. The thickness and proportion of carbon plies in the investigated hybrid layups were chosen to be in the Fragmentation and dispersed Delamination (Frag. & Del.) region to get the desired damage scenario.

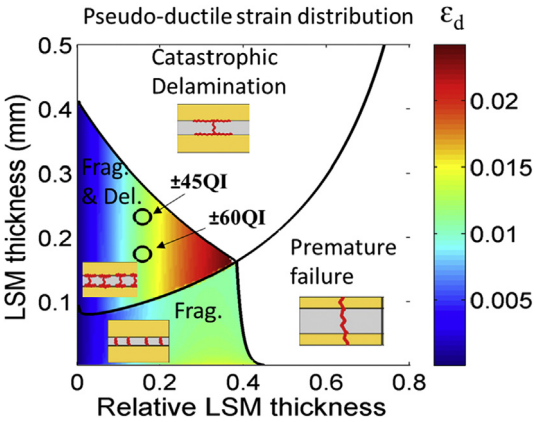

Fig. 4. Distribution of pseudo-ductile strain for the investigated ±60QI and ±45QI specimens.

2.2. Specimen manufacturing

The laminates were cured in an autoclave at the recommended cure temperature and pressure cycle for the Hexcel 913 resin (60 min at 125 °C, 0.7 MPa), which was also satisfactory for the carbon. Specimens were cut using a diamond-cutting wheel. The nominal specimen dimensions were 240/160/20/h mm overall length/free length/width/variable thickness respectively. End tabs made of 2 mm thick woven glass/epoxy plates supplied by Heathcotes Co. Ltd. were bonded to the specimens using a two component Araldite 2000 A/B epoxy adhesive supplied by Huntsman, the components were mixed with the volume fraction ratio of 100: 50 for A: B respectively and cured for 120 min at 80 °C inside a Carbolite oven. The final samples were visually inspected to assure appropriate quality. Good integrity of the hybrid laminates was confirmed during testing procedures and no phase separation was observed.

2.3. Test procedure

Tensile testing of the hybrid laminates was performed under uniaxial tensile loading and displacement control using a crosshead speed of 2 mm/min on a computer controlled Instron 8801 type 100 kN rated universal hydraulic test machine with wedge-type hydraulic grips. A 25 kN load cell was used for better resolution in the expected load range. At least 6 specimens of each type were tested to check the repeatability of the results. To measure the strains over a nominal gauge length of 130 mm, an Imetrum video gauge system was used by tracking a dotted pattern applied on the specimen face.

3. Results and discussion

3.1. Overall mechanical results

The desired pseudo-ductile response was achieved, with consistent stress-strain curves, without any catastrophic delamination and with obvious plateau as illustrated in Figs. 5–7. The carbon fibres started to fragment near the knee-point which was

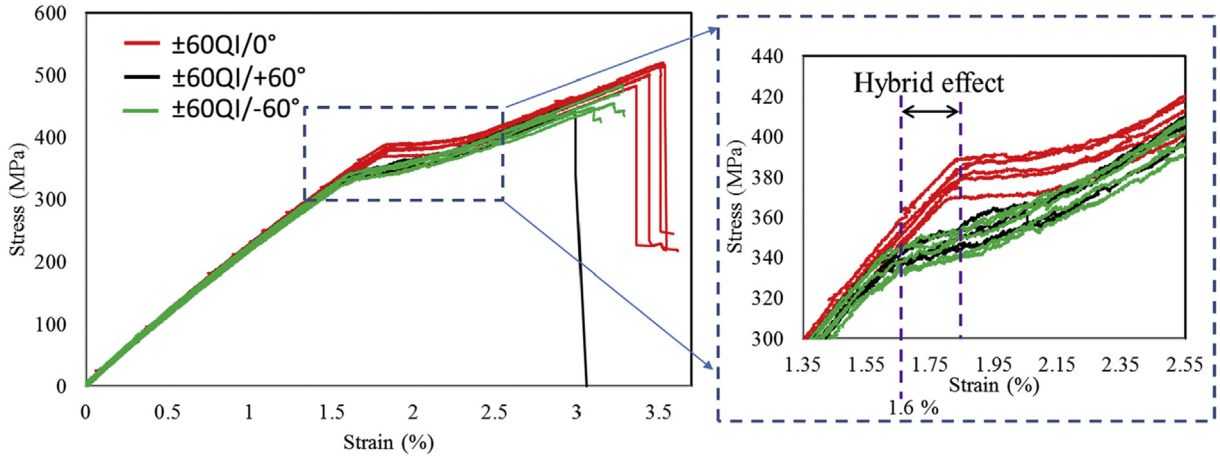

Fig. 5. Results of the tensile tests for the ±60QI specimens.

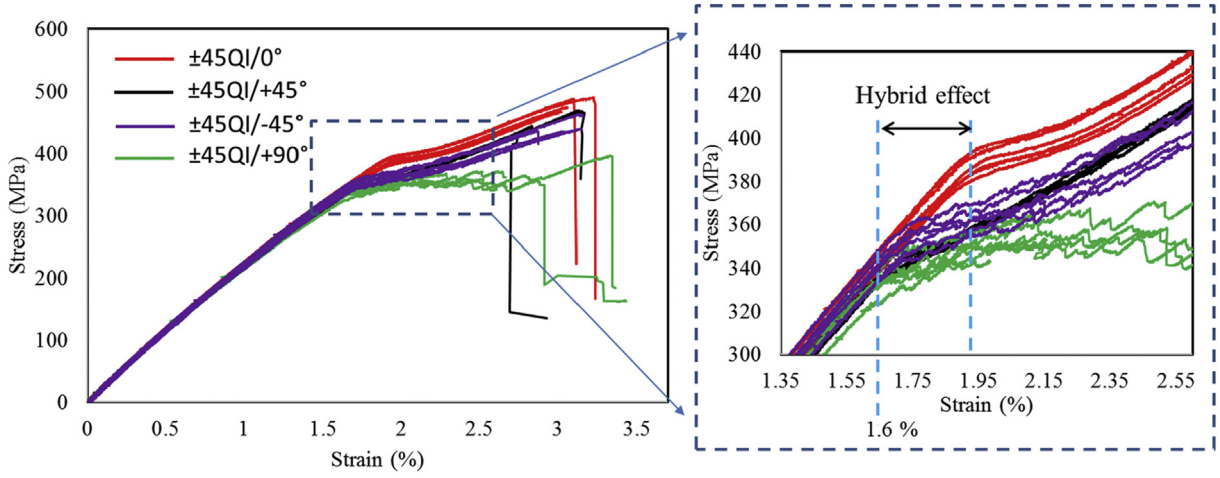

Fig. 6. Results of the tensile tests for the ±45QI specimens.

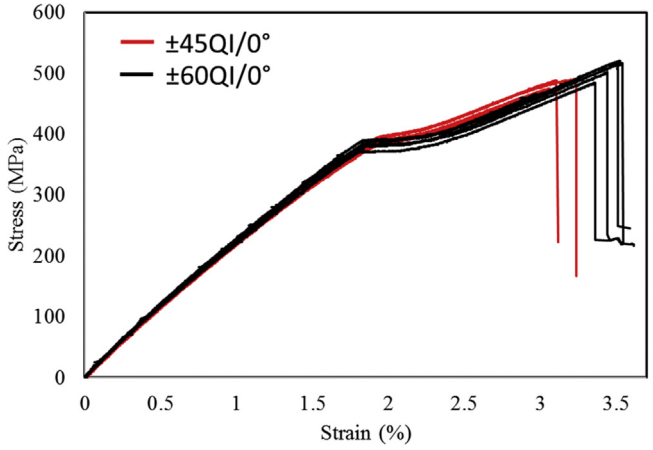

Fig. 7. Comparison of the tensile results for the ±45QI/0°and the ±60QI/0° specimens.

then followed by a plateau due to stable progressive carbon plies fragmentation and local delamination of the carbon fragments. After the plateau, the stress started to increase as fragmentation was fully saturated, the contribution of the carbon plies to the specimen stiffness was diminished and the glass plies carried most of the increase in load. The failure behaviour was in good agreement with that expected from the design considerations. It should be noted that the hybrid effect is not considered in the damage mode map results shown in Fig. 4, and the manufacturer's quoted failure strain for T300 carbon (1.5%) was used for the calculations.

Table 3 gives some of the important features of the curve such as the initial elastic modulus, pseudo-yield strain, and pseudo-ductile strain of these hybrid configurations. Pseudo-yield strain values were defined as the intersection of two lines fitted to the stress-strain graph before and after the fragmentation initiation point. The elastic response of the layups is identical, as expected; however, due to different hybrid effects, the average pseudo-yield strains and the average pseudo-yield stresses are slightly different.

3.2. Hybrid effect

It has been shown that the hybrid effect is strongly dependent on the ply thickness in UD hybrids [16]. As will be discussed in Section 3.3, the fragmentations appeared only in the 0° carbon plies. The thickness of single 0° carbon plies is the same for the ±45QI and ±60QI laminates, however they have different hybrid effects due to the different parameters such as numbers and stacking sequences of plies in the investigated configurations. The stiffness of the plies separating the two 0° carbon plies on either

Table 3
Summary of the test results for the hybrid specimens.

Specimen type	Initial in-plane elastic modulus (GPa)	Stiffness (modulus) of the plies separating 0° carbon plies N/mm (GPa)	Stiffness (modulus) of the outer ply adjacent to the 0° carbon ply N/mm (GPa)	Sum of the stiffness of the separator and adjacent layers N/mm	Pseudo-yield stress (MPa)	Relative stress-based hybrid effect (MPa)	Pseudo-yield strain (%)	Relative strain-based hybrid effect (%)	Pseudo -ductile strain (%)	Final failure strain (%)	Final failure stress (MPa)
±60QI/0°	23.5 ± 0.1	682 (5.88)	7083 (45.7)	7765	379 ± 6	45 (13.5%)	1.80 ± 0.02	0.2 (12.5%)	1.30 ± 0.05	3.5 ± 0.10	504 ± 18
±60QI/+60°	23.1 ± 0.2	–	170 (5.88)	170	334 ± 3	Reference	1.60 ± 0.04	Reference	1.15 ± 0.10	2.95 ± 0.15	436 ± 14
±60QI/-60°	23.2 ± 0.1	341 (5.88)	170 (5.88)	511	335 ± 7	1 (0.29%)	1.60 ± 0.02	0	1.20 ± 0.06	3.2 ± 0.10	464 ± 16
±45QI/0°	23.4 ± 0.1	2875 (16.52)	7083 (45.7)	9958	385 ± 7	51 (15%)	1.90 ± 0.03	0.3 (18.75%)	0.95 ± 0.06	3.10 ± 0.10	484 ± 8
±45QI/+45°	23.3 ± 0.1	–	256 (8.84)	256	335 ± 2	1 (0.29%)	1.65 ± 0.02	0.05 (3.13%)	1.05 ± 0.10	3.01 ± 0.22	441 ± 23
±45QI/+90°	23.2 ± 0.2	512 (8.84)	256 (8.84)	768	333 ± 5	–	1.62 ± 0.04	0.02 (1.25%)	1.46 ± 0.10	3.06 ± 0.20	343 ± 74
±45 QI/-45°	23.3 ± 0.2	1786 (15.38)	256 (8.84)	2042	350 ± 4	16 (4.8%)	1.70 ± 0.03	0.1 (6.25%)	0.96 ± 0.05	3.05 ± 0.15	441 ± 11

side of the symmetry plane and the stiffness of the outer plies adjacent to the 0° carbon plies are different for the various tested configurations, as illustrated schematically in Fig. 8. The stiffnesses of the separator plies and the adjacent plies are worked out using the mechanical properties listed in Table 1 and reported in Table 3. These stiffness values are evaluated by multiplying the modulus of the separator plies along the loading direction by the thickness of the plies. The shear deformation is constrained by the rest of the laminate, therefore, the longitudinal stiffness of the unbalanced 45_s and 60_s plies are considered to be the same as the balanced $\pm45_s$ and $\pm60_s$ plies, respectively. Since both the adjacent and separator plies are thought to influence the behaviour, a further column is included in Table 3 where these are added together. Although this is somewhat arbitrary, it does facilitate a comparison of their potential combined effect. For the ±60QI/0° and ±45QI/0° laminates, the nearby 0° glass ply has a significantly higher stiffness compared to the off-axis glass layers. So, when it is next to the fragmenting 0° carbon layer, the stress concentration at a single carbon fibre break would be lower as the glass ply can significantly contribute to carrying load around a subcritical cluster of broken fibres [21]. This explains the highest average pseudo-yield strain in the ±60QI/0° (1.80%) and the ±45QI/0° (1.90%) specimens. These strain values are significantly higher than the manufacturer's quoted 1.5% failure strain [25] and the pseudo-yield strain values for the other configurations listed in Table 3. The higher pseudo-yield strain in the ±45QI/0° laminate, compared to the ±60QI/0° laminate, is due to the thicker, stiffer and stronger separator laminate between the two 0° plies in these specimens. The higher ratio of the stiff 0° glass layer to the overall thickness in the ±60QI/0° results in a higher final failure strain, compared to the ±45QI/0° laminate. More

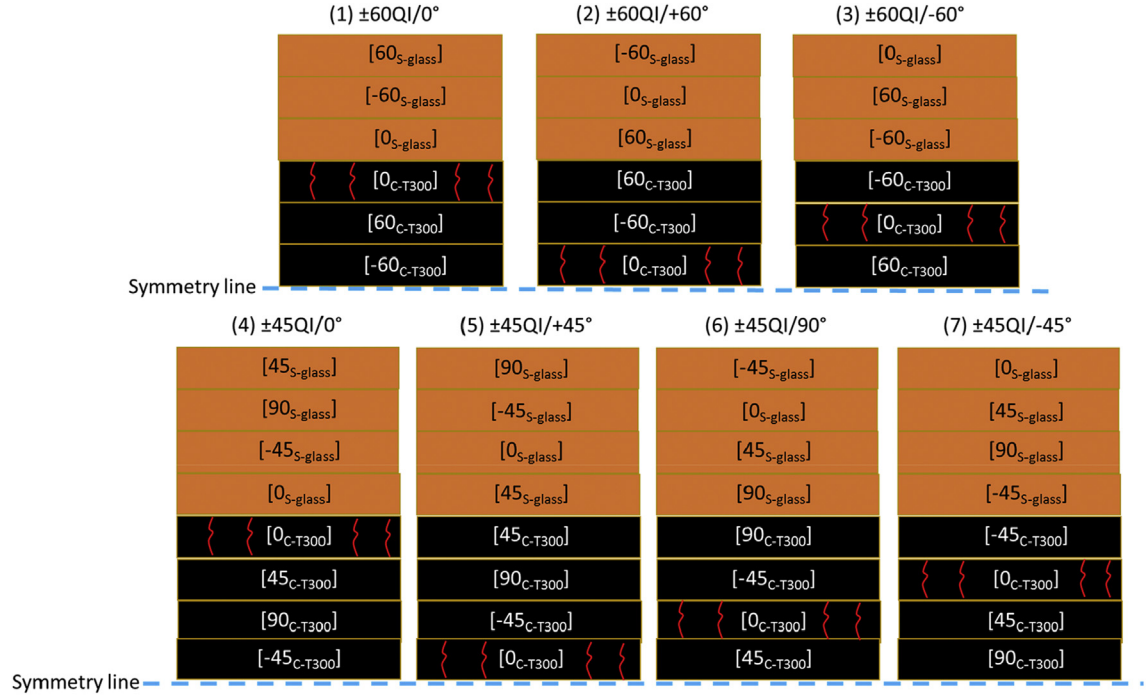

Fig. 8. Schematic of the investigated layups, the red lines on the 0° carbon plies are representative of fragmentations. (For interpretation of the references to colour in this figure legend, the reader is referred to the web version of this article.)

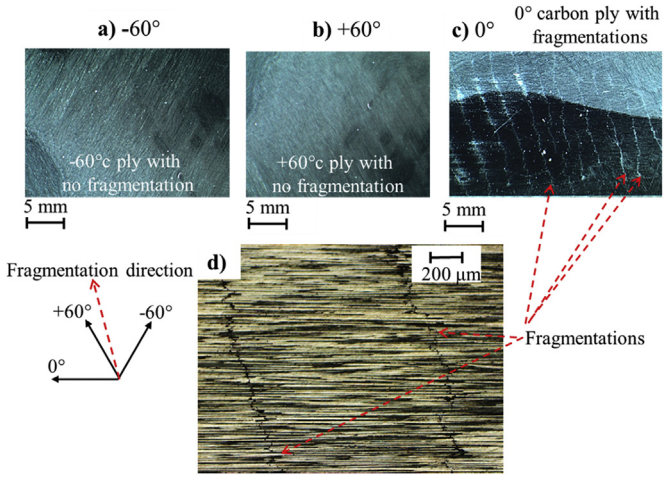

Fig. 9. Microscopy pictures from the polished surface of the ±60QI/-60° laminate at different depths through the thickness a) the −60° carbon ply with no fragmentation, b) the +60° carbon ply with no fragmentation, c) the 0° carbon ply with fragmentation and d) the 0° carbon ply, microscopy picture with higher zoom.

details can be found in Ref. [23].

For the other ±60QI and ±45QI laminates, the 0° carbon sub-laminate is adjacent to the ±60° and ±45° carbon layers with lower stiffness in the loading direction, respectively. Therefore, as listed in Table 3, the pseudo-yield strain values for these laminates is lower than the ±60QI/0° and ±45QI/0° laminates. Table 3 shows the different values for the hybrid effect of the investigated configurations. These values are measured relative to the ±60QI/+60° laminate that has the lowest hybrid effect. The pseudo-yield strain of ±60QI/+60° (1.6%) is higher than the manufacturer's quoted 1.5% failure strain [26]. The reason for this higher value is partially as a result of eliminating stress concentrations at the grips using the hybrid configuration that results in consistent gauge length failures, but may include a small hybrid effect as the 0° plies are still quite thin. Using the failure strain of ±60QI/+60° as the reference allows a comparison of the relative hybrid effects between the different layups. There is a need for further experimental, numerical and analytical investigations to study these hybrid effects more comprehensively.

3.3. Microscopic observations

Microscope top view images from specimens interrupted before the final failure, taken through the laminate thickness by grinding and polishing layers one-by-one from off the top, showed that the fragmentations were only in the 0° carbon plies. As an instance, Fig. 9 shows microscopy pictures from the polished surface of the ±60QI/-60° laminate at different depths through the thickness. Similar results were obtained for all the investigated specimens. Fig. 10 shows the fragmentation pattern in the 0° carbon layer over the width of the investigated layups after removing the top layers. The highest fragmentation crack density and pseudo-yield strain value (1.9%) with the smallest average fragmentation spacing is observed in the ±45QI/0° laminate which is believed to be due to the high combined stiffness of both the separator and adjacent plies (9958 N/mm). The ±60QI/0° laminate has the second-highest fragmentation cracks density and pseudo-yield strain value (1.8%) with the second-highest combined stiffness value (7765 N/mm). The ±45QI/-45° laminate has the third-highest combined stiffness value (2042 N/mm) and the third-highest pseudo-yield strain value (1.7%). The other ±60QI and ±45QI laminates, have significantly lower combined stiffness values compared with the ±60QI/0° and ±45QI/0° laminates. As a result, the fragmentation cracks densities in these laminates are lower than the ±60QI/0° and ±45QI/0° laminates. Another interesting observation is the angle of the oblique cracks in the 0° carbon layer. As shown in Fig. 10, the overall fragmentation path angle is oblique, and it is affected by the other carbon layers adjacent to the 0° carbon layer. The oblique angle is between the transverse direction and the orientation of the inner adjacent carbon layer. When the 0° carbon plies are in the mid-plane, the oblique angle is between the transverse direction and the orientation of the layers adjacent to the 0° carbon plies.

The location of the fragmentations in the investigated laminates are illustrated schematically in Fig. 8. By changing the location of

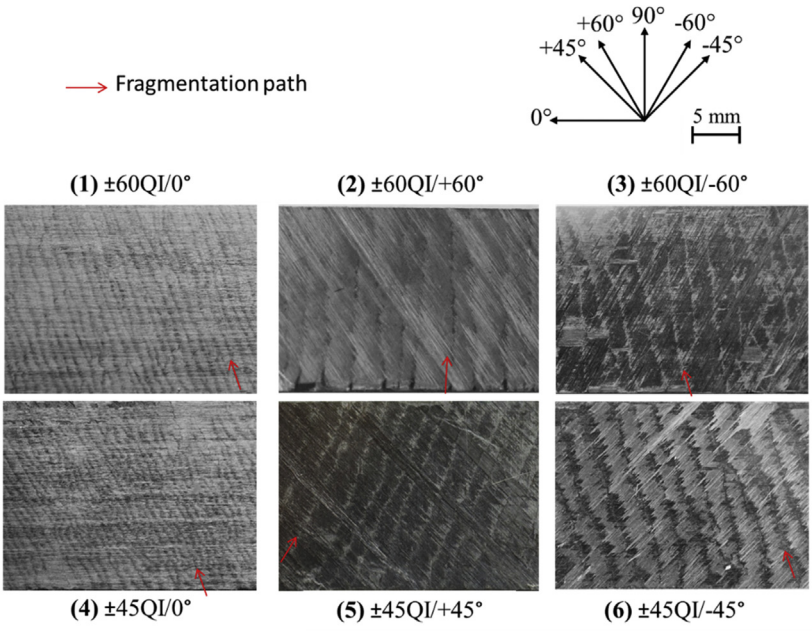

Fig. 10. Fragmentation pattern in the 0° carbon layer over the whole width of the investigated layups after removing the top layers.

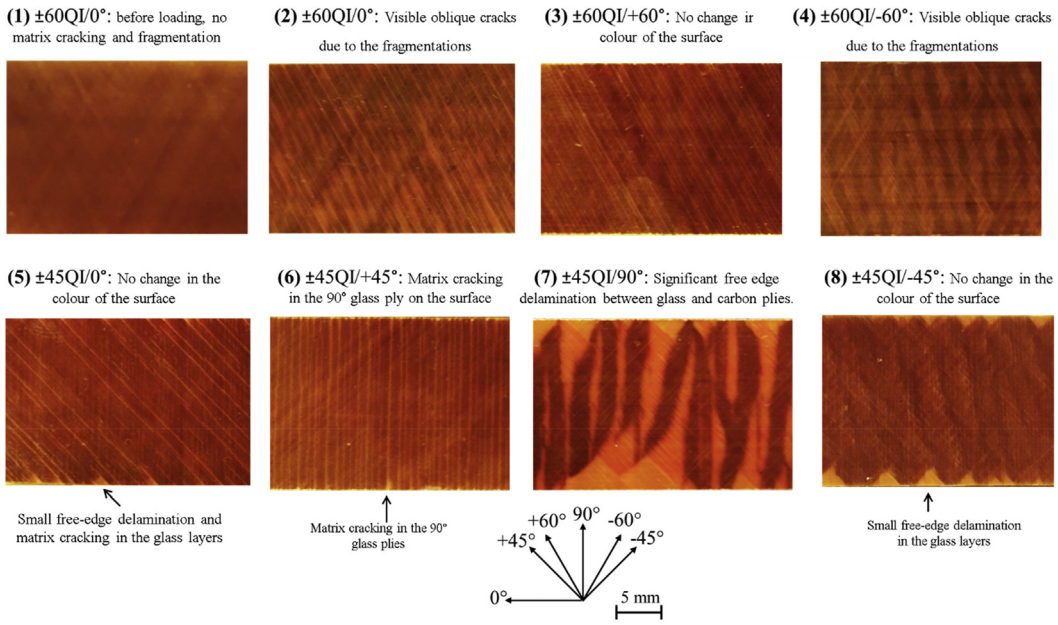

Fig. 11. Pictures from the top surface of the specimens before loading and interrupted tests, appearance of the specimen in different configurations for strain levels close to the final failure.

the 0° carbon plies, the damage location and mechanisms change, and as a result, the appearances of the laminates are different from each other as shown in Fig. 11. For the ±60QI/0° and ±60QI/-60° laminates, due to the translucent nature of the glass/epoxy composite on the outside of the hybrid laminate, well bonded areas appear to be black and clear oblique cracks are visible due to the fragmentations and dispersed delamination. However, the fragmentations in the ±60QI/+60° laminate are hidden by the other carbon layers, which were laid on top of the fragmented plies, and no visible crack (the surface colour change) was distinguished. The finer damage pattern in the ±45 QI/0°, illustrated in Fig. 10, is hardly visible through the thick glass layers (Fig. 11 (5)). For the ±45 QI/-45° and ±45 QI/+45°, the carbon plies covering the fragmentations hindered the visibility of the damage (Fig. 11 (6), (8)). The 90° glass layer is on the top of the ±45 QI/+45° laminate and the matrix cracking is clearly observable parallel to the fibres in this layer. It will be shown that the energy release rates are significantly higher in the ±45QI/+90° laminate, compared with the other laminates, which caused free-edge delaminations, just after a few carbon ply fragmentations, and resulted in the different appearance (Fig. 11 (7)) and the lowest final failure stress value (Fig. 6.).

3.4. Free-edge delamination

There was not any significant free-edge delamination for the investigated specimens except for the ±45 QI/90° specimen, hence the observable cracks on the ±45 QI/90° are due to the free-edge delaminations and fragmentations (See Fig. 12.). Free-edge delamination was observed after the first fragmentations within the carbon laminate. Even if there was significant free-edge delamination, no catastrophic load drop or overall delamination occurred. The reason behind the occurrence of the free-edge is the higher energy release rates at the free-edges of this layup due to the blocked 90° layers compared with the other laminates. A finite element slice modelling method that was developed in our previous studies [23] was used to show the importance of the stacking sequence on the energy release rates and to find the interfaces at which free-edge delamination would potentially propagate. The Abaqus Virtual Crack Closure Technique (VCCT) subroutine and 3D 8-noded brick elements (C3D8I) were used to calculate the energy release rates. The stress state does not vary along the length of the specimen for the regions far away from the end tabs. Therefore, a generalised plane strain solution was applied to avoid modelling the full length of a specimen.

Fig. 13 shows the failure index, defined as $G_I/G_{Ic} + G_{II}/G_{IIc} + G_{III}/G_{IIIc}$, calculated for delamination lengths of 5 mm at a far-field strain of 1% at all interfaces for the ±45QI/0° and ±45QI/+90°

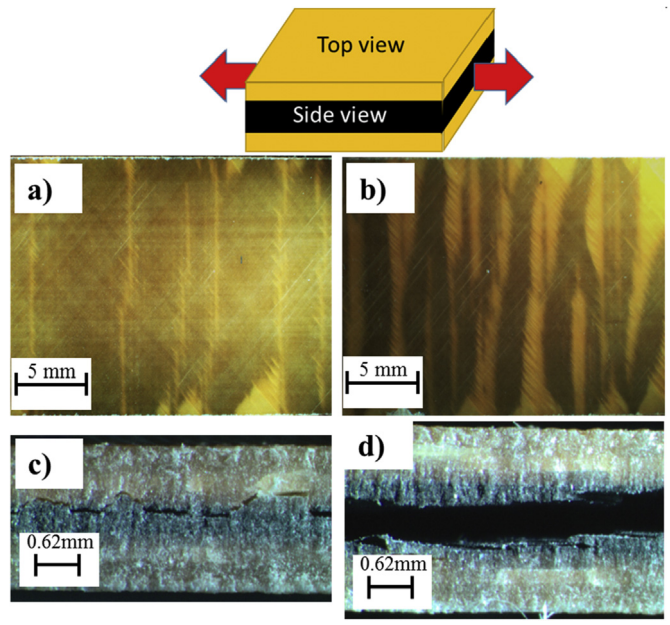

Fig. 12. Carbon-ply fragmentation for the interrupted ±45QI/+90° specimens a) Top view at 2.11% strain level and b) Top view at 2.65% strain level, c) Side view at 2.11% strain level and d) Side view at 2.65% strain level, the red arrows showing the loading direction. (For interpretation of the references to colour in this figure legend, the reader is referred to the web version of this article.)

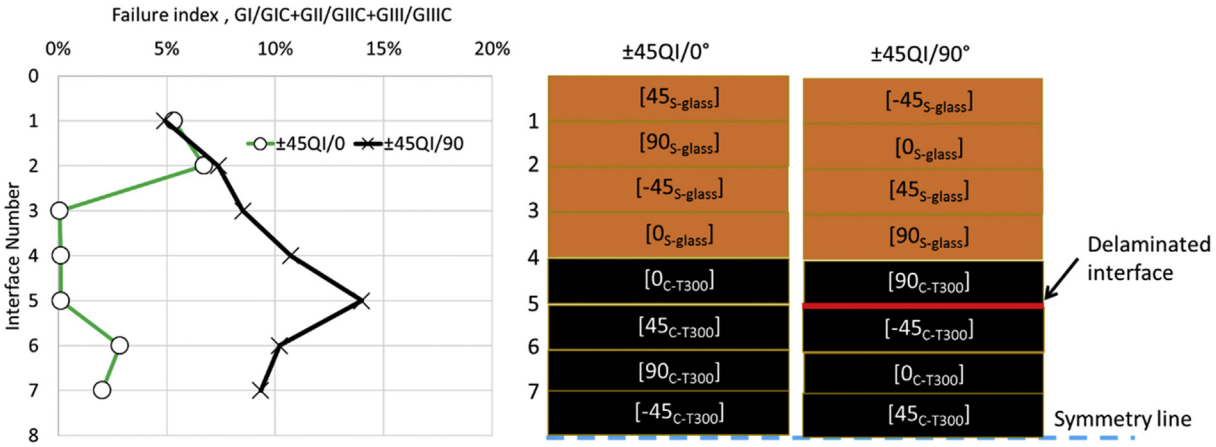

Fig. 13. Failure index, i.e. $G_I/G_{Ic}+(G_{II}+G_{III})/G_{IIc}$, for crack length of 5 mm at a far-field strain of 1% for the ±45QI/0° and ±45QI/+90° layups.

layups. Typical values of 0.2, 1.0 and 1.0 N/mm were used for G_{Ic}, G_{IIc} and G_{IIIc}, respectively. The assumed strain at which the failure indices are calculated is well below failure, hence the absolute values are relatively low. The failure indices are quite similar at interfaces 1 and 2 in both layups, whereas the failure indices are much larger for the other interfaces in the ±45QI/+90° layup compared to the ±45QI/0° layup. The failure index reaches its maximum value at interface 5 (around 14%), this interface is crucial for free-edge delamination. This is consistent with the experimental observations and the side view picture taken from the ±45QI/+90° layup illustrated in Fig. 12c, where free-edge delamination initiated at interface 5 after the first fragmentations within the carbon laminate.

4. Conclusions

The aim of this work was to generate high performance QI composite laminates that show pseudo-ductility in all the fibres orientations under tensile loading. This aim was successfully achieved by designing, manufacturing and testing novel QI thin-ply carbon/glass hybrid laminates. The laminates were made with orientation-dispersed layups in which non-hybrid multi-directional S-glass/epoxy and T300-carbon/epoxy sub-laminates were put together to build the hybrid laminate. The following conclusions are drawn:

1. The investigated QI laminates showed the desired pseudo-ductility in all the fibre directions, with an obvious plateau and without any catastrophic delamination before the final failure. The orientation-dispersed concept successfully suppressed free-edge delamination, which was an unwanted damage mode in the previously investigated QI laminates fabricated using the orientation-blocked concept. Pseudo-ductile strains of up to 1.3% were achieved, with strengths up to 504 MPa.
2. Microscopic observation showed carbon ply fragmentations just in the 0° carbon plies with overall fragmentation path angles that are oblique. The angle is affected by the other carbon layers adjacent to the 0° carbon layer, and is between the transverse direction and the orientation of the adjacent carbon layers.
3. A significant hybrid effect was observed, with a pseudo-yield strain corresponding to carbon ply failure of 1.90% for the ±45QI laminates with the 0 carbon plies adjacent to the 0 glass plies, compared with only 1.6% in some of the other ±60QI configurations. The effect was found to be dependent on the stiffness of the inner plies separating the 0° carbon plies and the plies adjacent to the 0° carbon plies. Altering the stacking sequence influences the stiffness of the separator and adjacent plies, therefore, leads to changes in the pseudo-yield strain and final failure stress/strain.

Acknowledgements

This work was funded under the UK Engineering and Physical Sciences Research Council (EPSRC) Programme Grant EP/I02946X/1 on High Performance Ductile Composite Technology in collaboration with Imperial College, London. The authors acknowledge Hexcel Corporation for supplying materials for this research. The authors would like to thank Mr Guillermo Idarraga for his help in processing the data. The data necessary to support the conclusions are included in the paper.

References

[1] N.L. Hancox, Fibre Composite Hybrid Materials, Applied Science Publishers Ltd., London, 1981.
[2] J. Summerscales, D. Short, Carbon fibre and glass fibre hybrid reinforced plastics, Composites 9 (1978) 157–166.
[3] D. Short, J. Summerscales, Hybrids – a review Part 1. Techniques design and construction, Composites 10 (1979) 215–221.
[4] D. Short, J. Summerscales, Hybrids – a review Part 2. Physical properties, Composites 11 (1980) 33–38.
[5] G. Kretsis, A review of the tensile, compressive, flexural and shear properties of hybrid fibre-reinforced plastics, Composites 18 (1987) 13–23.
[6] G. Marom, S. Fischer, F.R. Tuler, H.D. Wagner, Hybrid effects in composites: conditions for positive or negative effects versus rule-of-mixtures behaviour, J. Mater Sci. 13 (7) (1978) 1419–1426.
[7] N. Svensson, Manufacturing of thermoplastic composites from commingled yarns – a review, J. Thermoplast. Compos Mater 11 (1) (1998) 22–56.
[8] H. Diao, A. Bismarck, P. Robinson, M.R. Wisnom, Pseudo-ductile behaviour of unidirectional fibre reinforced polyamide-12 composite by intra-tow hybridization, in: Proceedings of ECCM 15 Conference. Venice, June, 2012.
[9] T. Hayashi, Development of new material properties by hybrid composition. 1st report, Fukugo Zair. Compos. Mater. 1 (1972) 18–20.
[10] T. Hayashi, K. Koyama, A. Yamazaki, M. Kihira, Development of new material properties by hybrid composition. 2nd report, Fukugo Zair. Compos. Mater. 1 (1972) 21–25.
[11] A.R. Bunsell, B. Harris, Hybrid carbon and glass fibre composites, Composites 5 (1974) 157–164.
[12] J. Aveston, J.M. Sillwood, Synergistic fiber strengthening in hybrid composites, J. Mater Sci. 11 (10) (1976) 1877–1883.
[13] P.W. Manders, M.G. Bader, The strength of hybrid glass/carbon fibre composites, J. Mater Sci. 16 (1981) 2233–2245.
[14] T. Yokozeki, Y. Aoki, T. Ogasawara, Experimental characterization of strength and damage resistance properties of thin-ply carbon fiber/toughened epoxy laminates, Compos Struct. 82 (2008) 382–389.
[15] H. Saito, M. Morita, K. Kawabe, et al., Effect of ply-thickness on impact damage morphology in CFRP laminates, J. Reinf. Plast. Compos 30 (2011) 1097–1106.
[16] T. Yokozeki, A. Kuroda, A. Yoshimura, T. Ogasawara, T. Aoki, Damage

characterization in thin-ply composite laminates under out-of-plane transverse loadings, Compos Struct. 93 (2010) 49–57.
[17] G. Czél, M.R. Wisnom, Demonstration of pseudo-ductility in high performance glass-epoxy composites by hybridisation with thin-ply carbon prepreg, Compos Part A Appl. Sci. Manuf. 52 (2013) 23–30.
[18] M. Jalalvand, G. Czél, M.R. Wisnom, Damage analysis of pseudo-ductile thin-ply UD hybrid composites – a new analytical method, Compos Part A 69 (2015) 83–93.
[19] M. Fotouhi, P. Suwarta, M. Jalalvand, G. Czel, M.R. Wisnom, Detection of fibre fracture and ply fragmentation in thin-ply UD carbon/glass hybrid laminates using acoustic emission, Compos. Part A Appl. Sci. Manuf. 86 (2016) 66–76.
[20] Y. Swolfs, L. Gorbatikh, I. Verpoest, Fibre hybridisation in polymer composites: a review, Compos. Part A 67 (2014) 181–200.
[21] M.R. Wisnom, G. Czél, Y. Swolfs, M. Jalalvand, L. Gorbatikh, I. Verpoest, Hybrid effects in thin ply carbon/glass unidirectional laminates: accurate experimental determination and prediction, Compos Part A 88 (2016) 131–139.
[22] G. Czél, T. Rév, M. Jalalvand, M. Fotouhi, MR. Wisnom. Demonstration of pseudoductility in quasi-isotropic laminates comprising thin-ply UD carbon/epoxy hybrid sublaminates, ECCM17 17th European Conference on Composite Materials (Munich, 26–30 June 2016).
[23] M. Jalalvand, M. Fotouhi, G. Czél, MR. Wisnom. Avoiding free edge delamination in Quasi-Isotropic pseudo-ductile hybrid laminates – by material dispersion or layer angle dispersion? ECCM17 17th European Conference on Composite Materials (Munich, 26–30 June 2016).
[24] S.R. Hallett, M.R. Wisnom, Numerical investigation of progressive damage and the effect of layup in notched tensile tests, J. Compos Mater 40 (2005) 1229–1245.
[25] T300 Data Sheet - No. CFA-001. n.d. (http://www.toraycfa.com/pdfs/T300DataSheet.pdf).
[26] J. Fuller, M.R. Wisnom, Damage suppression in thin ply angle-ply carbon/epoxy laminates, in: 19th Int. Conf. Compos. Mater., Montreal, 2013.